MCEN90028 Robotics Systems Assignment 1 Report

Group 3

Hai Dang Nguyen 860308
Say Ee See 813641
BhargavRam Chilukuri 964069

4/3/2021

Contents

1 Introduction **2**

2 Forward Kinematics **3**
2.1 Robot Schematic Diagram . . . 3
2.2 Denavit–Hartenberg (DH) Table and transformation matrices . . . 3
2.3 Analysis of Forward Kinematics . . . 4
2.4 Determination of Link Lengths . . . 6
2.4.1 First attempt . . . 6
2.4.2 Analysis . . . 7
2.4.3 Second attempt . . . 8

3 Inverse Kinematics **10**
3.1 Inverse Kinematics solution . . . 10
3.1.1 Q_1 solution . . . 10
3.1.2 Q_2, Q_3, Q_4 solution . . . 10
3.2 Inverse Kinematics Verification . . . 12

4 Conclusion **16**

List of Figures

1 Robot for moving chess pieces . . . 2
2 Schematic of robot in “zero” position . . . 3
3 Stick figure plot of robot configurations . . . 5
4 Reachable space of the robot with initialised parameters . . . 7
5 Work Space sketch . . . 8
6 Reachable space of the robot (Top View & Side View) . . . 9
7 Side View on XZ plane of the robot and chessboard . . . 9
8 Top View of the robot . . . 10
9 Side View of the robot . . . 11
10 Inverse Kinematics Results for r_1 . . . 13
11 Inverse Kinematics Results for r_2 . . . 14
12 Configuration 2 and 3 . . . 14
13 Configuration 4 and 5 . . . 15
14 Configuration 1 . . . 15

List of Tables

1 DH Table . . . 3
2 Physical parameters and Joint displacement range (First attempt) . . . 6
3 Physical parameters and Joint displacement range (Second attempt) . . . 8
4 Inverse Kinematics Results for r_1 = [170;0;10;1] . . . 12
5 Inverse Kinematics Results for r_2 = [110;65 ;20;1] . . . 13

1 Introduction

The project aims to create a robot that can automatically move pieces in a chess game. As the first part of the design process, this report will investigate the relationship of the robot arm's properties and its capability to complete the task. This implies that the reachable workspace of the robot need to cover the entire playable area of the chessboard (130 x 130 mm), as shown in figure 1. The following objectives will be explicitly addressed throughout the report:

- Derive the output of end-effector pose as a function of joint displacements and physical parameters of the robot, using the Denavit-Hartenberg convention.
- Derive the output of joint displacements as a function of the end-effector pose and physical parameters.
- Determine the link lengths of the robot such that it can reach to the necessary workspace.
- Evaluate and validate the outcome from the first three objectives.

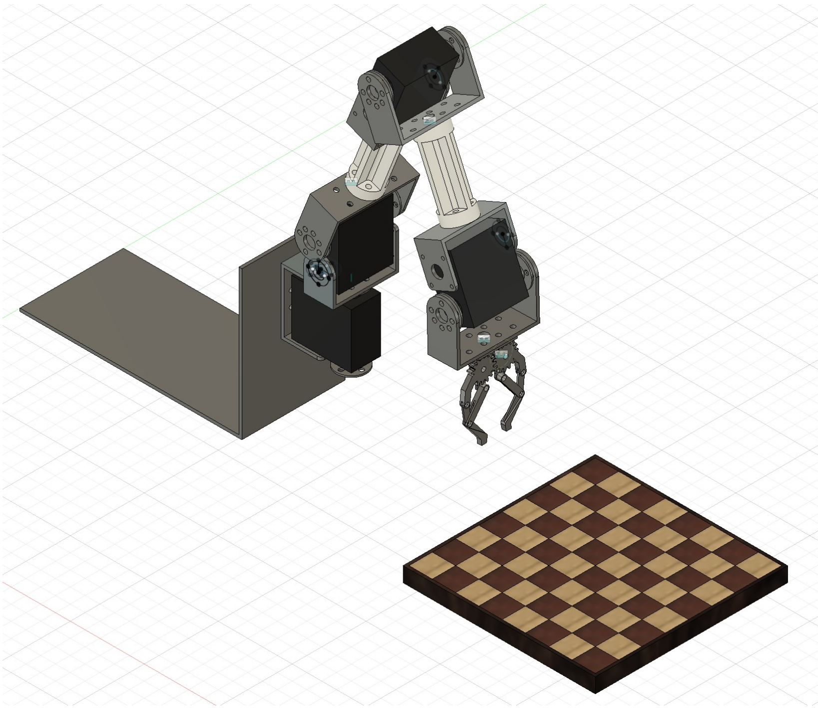

Figure 1: Robot for moving chess pieces

2 Forward Kinematics

2.1 Robot Schematic Diagram

Assuming the robot is in"zero" position i.e. with all rotational angles at the joints set to 0, we can produce the following schematic diagram:

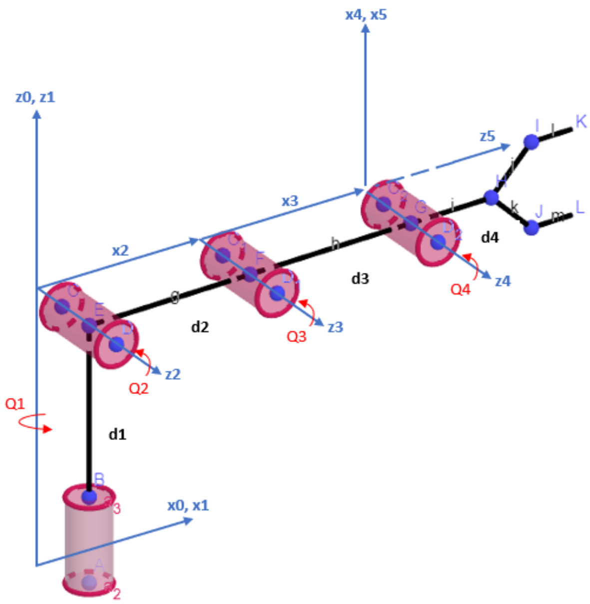

Figure 2: Schematic of robot in "zero" position

The robotic arm has 4 degrees of freedom, as illustrated by the rotational angles Q1-Q4. The length of the connecting shafts are represented by d1-d4, and the reference frames (x_0-x_5, z_0-z_5) are shown attached to their respective revolute joints and the end effector.

2.2 Denavit–Hartenberg (DH) Table and transformation matrices

To determine the forward kinematics of our robot, we will utilise the Denavit-Hartenberg parameters to construct the DH table shown:

Table 1: DH Table

i	a_{i-1}	α_{i-1}	d_i	Q_i
1	0	0	d_1	Q_1
2	0	$\pi/2$	0	Q_2
3	d_2	0	0	Q_3
4	d_3	0	0	$Q_4+\pi/2$
5	0	$\pi/2$	d_4	0

A detailed explanation of how the frames and corresponding DH table parameters were determined is provided in section 2.3. Using our Denavit-Hartenberg parameters, we can now derive our transformation matrices using the equation below:

$$ {}^{i-1}_{i}T = D_x(a_{i-1}) \,.\, R_x(\alpha_{i-1}) \,.\, D_z(d_i) \,.\, R_z(Q_i), \;\; i = 1, 2...5 \tag{1}$$

whereby:

$$D_x(r) = \begin{bmatrix} 1 & 0 & 0 & r \\ 0 & 1 & 0 & 0 \\ 0 & 0 & 1 & 0 \\ 0 & 0 & 0 & 1 \end{bmatrix}, \; R_x(\theta) = \begin{bmatrix} 1 & 0 & 0 & 0 \\ 0 & \cos\theta & -\sin\theta & 0 \\ 0 & \sin\theta & \cos\theta & 0 \\ 0 & 0 & 0 & 1 \end{bmatrix}$$

$$D_z(r) = \begin{bmatrix} 1 & 0 & 0 & 0 \\ 0 & 1 & 0 & 0 \\ 0 & 0 & 1 & r \\ 0 & 0 & 0 & 1 \end{bmatrix}, \; R_z(\theta) = \begin{bmatrix} \cos\theta & -\sin\theta & 0 & 0 \\ \sin\theta & \cos\theta & 0 & 0 \\ 0 & 0 & 1 & 0 \\ 0 & 0 & 0 & 1 \end{bmatrix}$$

To obtain the transformation matrix of frame E (x_5, y_5, z_5) attached at the end effector with respect to Frame 0 (x_0, y_0, z_0) at the base of the manipulator, we simply multiply our obtained transformation matrices of frame i with respect to frame $i-1$ in the following sequence:

$$\begin{aligned} {}^0_ET &= {}^0_1T \cdot {}^1_2T \cdot {}^2_3T \cdot {}^3_4T \cdot {}^4_5T \\ &\simeq \begin{bmatrix} \sigma_{11} & \sin(Q_1) & \sigma_{13} & \sigma_{14} \\ \sigma_{21} & -\cos(Q_2) & \sigma_{23} & \sigma_{24} \\ \cos(Q_2+Q_3+Q_4) & 0 & \sin(Q_2+Q_3+Q_4) & \sigma_{34} \\ 0 & 0 & 0 & 1 \end{bmatrix} \end{aligned} \tag{2}$$

where:

$$\begin{aligned} \sigma_{11} &= -0.5\sin(Q_2 - Q_1 + Q_3 + Q_4) - 0.5\sin(Q_1 + Q_2 + Q_3 + Q_4) \\ \sigma_{13} &= 0.5\cos(Q_2 - Q_1 + Q_3 + Q_4) + 0.5\cos(Q_1 + Q_2 + Q_3 + Q_4) \\ \sigma_{14} &= \cos(Q_1) * \big(d_3\cos(Q_2 + Q_3) + d_2\cos(Q_2) + d_4\cos(Q_2 + Q_2 + Q_4)\big) \\ \sigma_{21} &= 0.5\cos(Q_1 + Q_2 + Q_3 + Q_4) - 0.5\cos(Q_2 - Q_1 + Q_3 + Q_4) \\ \sigma_{23} &= 0.5\sin(Q_1 + Q_2 + Q_3 + Q_4) - 0.5\sin(Q_2 - Q_1 + Q_3 + Q_4) \\ \sigma_{24} &= \sin(Q_1) * \big(d_3\cos(Q_2 + Q_3) + d_2\cos(Q_2) + d_4\cos(Q_2 + Q_3 + Q_4)\big) \\ \sigma_{34} &= d_1 + d_3\sin(Q_2 + Q_3) + d_2\sin(Q_2) + d_4\sin(Q_2 + Q_3 + Q_4) \end{aligned}$$

2.3 Analysis of Forward Kinematics

To validate our forward kinematics solution, we will first discuss how the DH table was derived. Setting our initial reference frame (x_0, z_0) at the base of the robot, we can obtain the Denavit-Hartenberg parameters through the following steps:

- Attach reference frame (x_1, z_1) to bottom leftmost revolute joint, 1st component of transformation is a translation by d_1 and a rotation by Q_1 about z_1
- Attach reference frame (x_2, z_2) to top leftmost revolute joint, 2nd component of transformation is a rotation by $\pi/2$ about x_1 and a rotation by Q_2 about z_2
- Attach reference frame (x_3, z_3) to top middle revolute joint, 3rd component of transformation is a translation by d_2 about x_2 and a rotation by Q_3 about z_3
- Attach reference frame (x_4, z_4) to rightmost revolute joint, 4th component of transformation is a translation by d_3 about x_3 and a rotation by $Q_3 + \pi/2$ about z_4
- Attach reference frame (x_5, z_5) to rightmost revolute joint, 5th component of transformation is a translation by d_4 about z_5 and a rotation by $\pi/2$ about x_4. Note that this transformation is to ensure that the end-effector is always pointing in the -z direction.

To test if our Denavit-Hartenberg parameters correctly represent the forward kinematics of the robot, we can plot the robot configuration for both the zero position - **Configuration 1** $(Q_1, Q_2, Q_3, Q_4 = 0)$ and when the end-effector is pointing downwards on the x_0-y_0 plane - **Configuration 2** $(Q_1, Q_2, Q_3 = 0,\ Q_4 = {}^{-\pi}/_{2})$. The coordinates of the robot's revolute joints $(r_i,\ i = 1, 2, 3, 4)$ and end-effector e are derived as follows:

For origin $O =$ [0;0;0;1], $d_1, d_2, d_3 = 200\,mm$, $d_4 = 80\,mm$:

$$
\begin{aligned}
r_1 &= O \\
r_2 &= {}^0_1T * O \\
r_3 &= {}^0_1T * {}^1_2T * {}^2_3T * O \\
r_4 &= {}^0_1T * {}^1_2T * {}^2_3T * {}^3_4T * O \\
r_5 = e &= {}^0_1T * {}^1_2T * {}^2_3T * {}^3_4T * {}^4_5T * O
\end{aligned}
$$

The transformation matrix of frame 5 attached to the end-effector with respect to frame 0 for both configurations are obtained

$$
\text{Configuration 1: } {}^0_5T = \begin{bmatrix} 0 & 0 & 1 & 480 \\ 0 & -1 & 0 & 0 \\ 1 & 0 & 0 & 200 \\ 0 & 0 & 0 & 1 \end{bmatrix}, \quad \text{Configuration 2: } {}^0_5T = \begin{bmatrix} 1 & 0 & 0 & 400 \\ 0 & -1 & 0 & 0 \\ 0 & 0 & -1 & 120 \\ 0 & 0 & 0 & 1 \end{bmatrix}
$$

We then plot the obtained coordinates using MATLAB to obtain the following result:

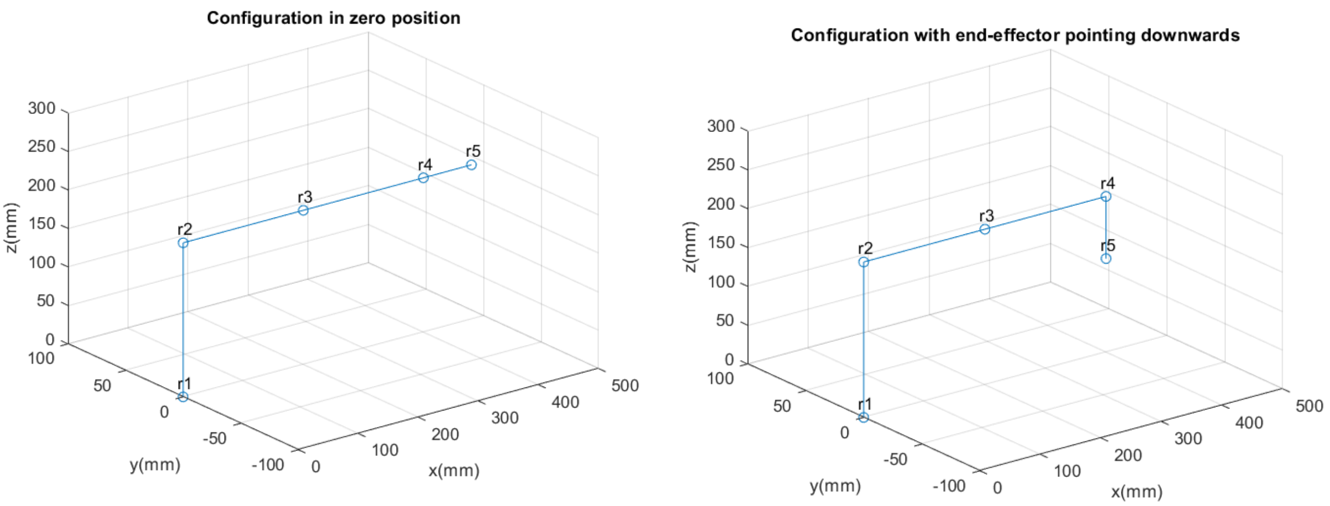

Figure 3: Stick figure plot of robot configurations

The plots in Figure 3 correctly show the robot in the aforementioned configurations, hence our derived forward kinematics solution are correct.

2.4 Determination of Link Lengths

2.4.1 First attempt

Having Forward Kinematics result, for a given link lengths and joint displacements, the position of joints can be identified with the respect to the inertial frame. Link lengths can be determined based on trial-and-error and chosen to ensure the furthest and shortest spots on the chessboard can be reachable.

Table 2 shows the initial guess values for physical parameters and joint displacements.

Table 2: Physical parameters and Joint displacement range (First attempt)

Physical properties	**Value (mm)**	**Joint displacement**	**Value (rad)**
d_1	30	Q_1	$[-\pi/4,\ \pi/4]$
d_2	98	Q_2	$[\pi/36,\ 0.59\pi]$
d_3	98	Q_3	$[-\pi/36,\ -3\pi/4]$
d_4	30	Q_4	$[0,\ -\pi/2]$

The aim of this study is to make sure the the chessboard can lie in the working range of the robot, which needs to be viewed from the top (XY plane in frame 0) and side (XZ plane in frame 1 at $Q_1 = 0$). Assuming that the required contact point for picking up the chess piece is 20 mm above the surface and the required height for translating chess pieces is 3 times the chess piece's height (assuming it is 30 mm), which is 90 mm above the surface. Therefore, in order to determine the reachable space of the arm, it is necessary to plot the pose of the end-effector on XY plane at Z = 20 mm and 90 mm for ensuring the capability of picking up and translating the chess piece at any requested point on the board.

The coordinates of the end-effector is being identified by using Forward Kinematics with different values of Q_2 and Q_3, whereas, Q_4 will be calculated from Q_2, Q_3 such that either it is $-\pi/2$ or the link d_4 always points vertically downwards for ease of picking the chess piece. There are 75 equal-spaced joint displacements in each value range associated with Q_1, Q_2, Q_3 to be selected representing different possible poses of the end-effector in space. Using MATLAB, the result of this study using the first guess physical properties is shown in Figure 4.

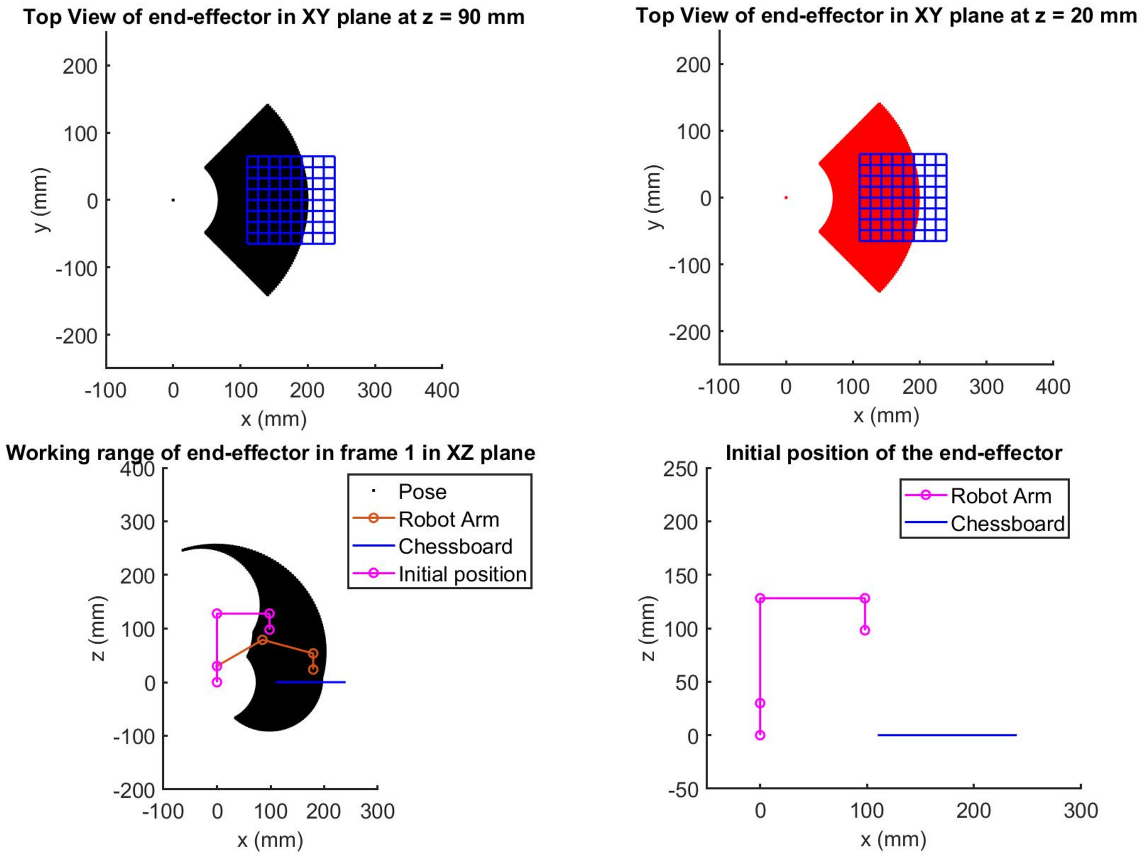

Figure 4: Reachable space of the robot with initialised parameters

Observing the plot, the chess board is not fully covered by the end-effector pose, which indicates that the link length is not long enough for the robot to reach to every spot on the chess board. Rather than incrementally increasing the link length, an analysis will be conducted to identify the minimum and maximum link length needed for reaching to the furthest and shortest location on the board.

2.4.2 Analysis

From the sketch in Figure 5, the furthest spot the robot arm needs to reach to is the far top and bottom corner of the chessboard. Moreover, the shortest range would be the perpendicular distance from d_1 to the nearest chessboard's edge, which is 110 mm plane-wise. These two configurations can be precisely viewed from the side view of the Figure 5, where OABC and OADE present the configuration of the robot arm for reaching to the shortest and furthest point respectively. In the OADE configuration, the joint displacement Q_2, Q_3 are limited to be $\pi/36$ from the zero position. Whereas, for OABC configuration, Q_3 is limited to $3\pi/4$ from zero position due to mechanical limitation of the bracket and motor.

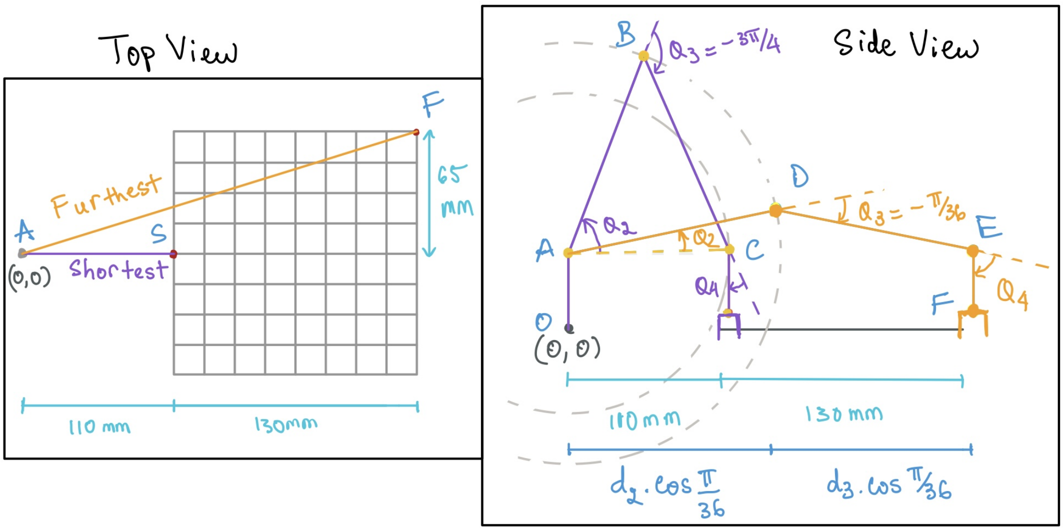

Figure 5: Work Space sketch

For configuration OADE, the minimum projected length of the robot arm in XY plane at Z = 0 is: $AF = \sqrt{240^2 + 65^2} = 248.64\ mm$. Assuming that $d_2 = d_3$ then $d_2 = d_3 \geq 248.64 \times 0.5 \times [cos(\pi/36)]^{-1} = 124.8\ mm$. Hence, the minimum link length is 124.8 mm.

For configuration OABC, to reach to the shortest point on the board, this condition must be met: $AC \leq AS = 110mm$. Using cosine rule in ABC for calculating AC, we have

$$\begin{aligned} AC &= \sqrt{AB^2 + BC^2 - 2.AB.BC.cos(\pi/4)} \\ &= \sqrt{2d_2^2 - \sqrt{2}d_2^2} \leq 110 \\ \therefore d_2 &\leq 143.7mm \end{aligned}$$

From the analysis, the suitable value range of d_2, d_3 is $124.8 \leq d_2 = d_3 \leq 143.7mm$.

2.4.3 Second attempt

The table 3 presents the assigned parameter values for the second attempt. $d_2,\ d_3$ are chosen to be 138 mm whereas $d_1 = d_4 = 50\ mm$.

Table 3: Physical parameters and Joint displacement range (Second attempt)

Physical properties	**Value (mm)**	**Joint displacement**	**Value (rad)**
d_1	50	Q_1	$[-\pi/4,\ \pi/4]$
d_2	138	Q_2	$[\pi/36,\ 0.59\pi]$
d_3	138	Q_3	$[-\pi/36,\ -3\pi/4]$
d_4	50	Q_4	$[0,\ -\pi/2]$

For each value of the joint displacement, the end-effector pose is plotted accordingly along with the chessboard, presented in Figure 6. From the top view, the chessboard is entirely fitted in the working range of the robot arm. The length of the link was chosen such that every point on the chessboard is reachable. Whereas from the side view, the arm can reach almost up to 150 mm above the chessboard. As the end-effector needs to point vertically downward during the task, its length should be long enough for ease of picking the chess piece yet short enough not to hit other chess pieces while translating.

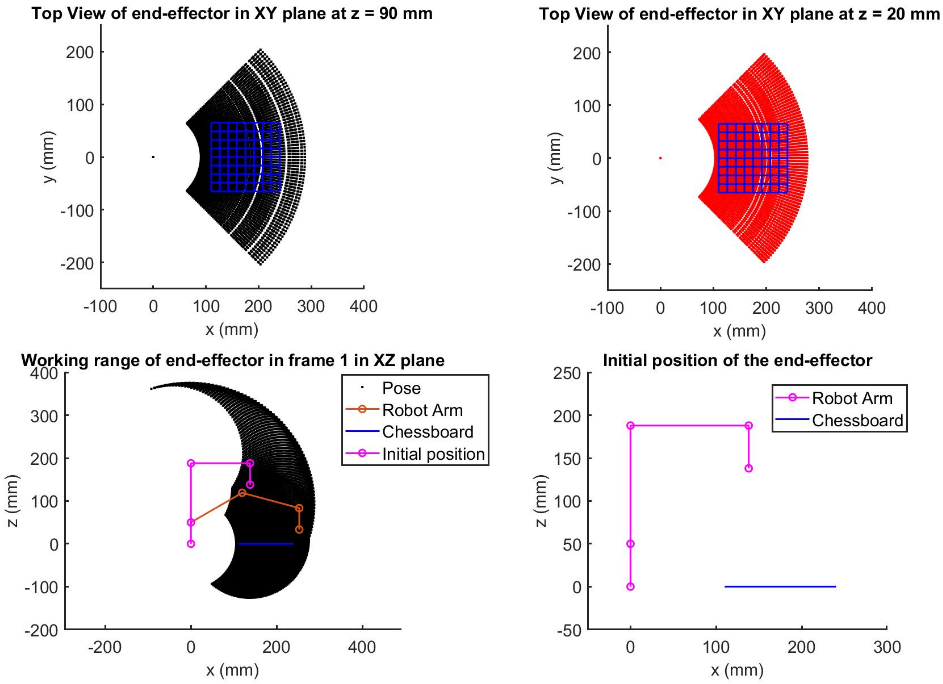

Figure 6: Reachable space of the robot (Top View & Side View)

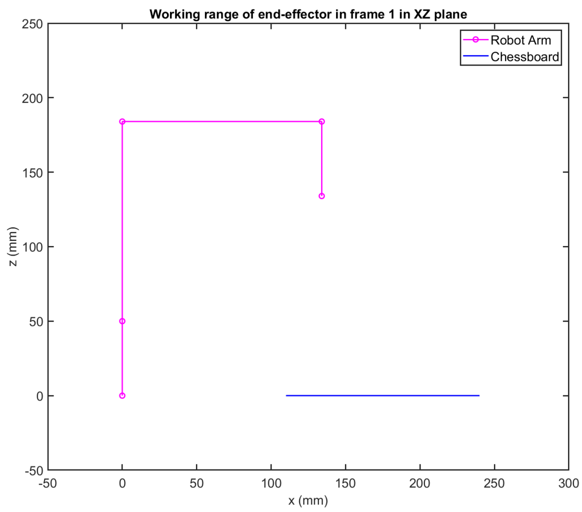

Figure 7: Side View on XZ plane of the robot and chessboard

The link length is chosen to be not too short nor too long due to the following reasons. There are uncertainty in the motor electronics components and the mechanical dimension of the bracket and motors, so there is no clue to guarantee that the motor can precisely rotate to the requested angle to reach to the furthest and shortest location on the board. Having a not too short nor too long link means that we weight both uncertainties equally, allowing more working range to counter the uncertainties. Moreover, have a too long link will add more weight to the overall structure of the arm, forcing the motor at joint Q_1, Q_2 to operate at a higher power in order to produce enough torque to rotate the structure, which can accumulate to a huge cost in power consumption considering a larger scale and number of robot arms for such an application like pick-and-drop in a warehouses or manufactories.

3 Inverse Kinematics

3.1 Inverse Kinematics solution

The objective of this section is solving for the joint displacement $[Q_1, Q_2, Q_3, Q_4]$ from the given position (x, y, z) of the end-effector in frame 0. From Figure 2, the robot arm consists of 4 links, (d_1, d_2, d_3, d_4), while d_1, d_2, d_3 with associated joint displacements help to navigate the chess piece position, d_4 helps to keep the z axis of the end-effector veritcally downwards. Therefore, the solution will be proceeded in sequence: solve for Q_1 then solve for Q_2, Q_3 and the last will be for Q_4.

3.1.1 Q_1 solution

From the top view projection of the robot on the x_0-y_0 plane (Figure 8), joint displacement Q_1 can be calculated as.

$$Q_1 = \tan^{-1} \frac{y}{x} \tag{3}$$

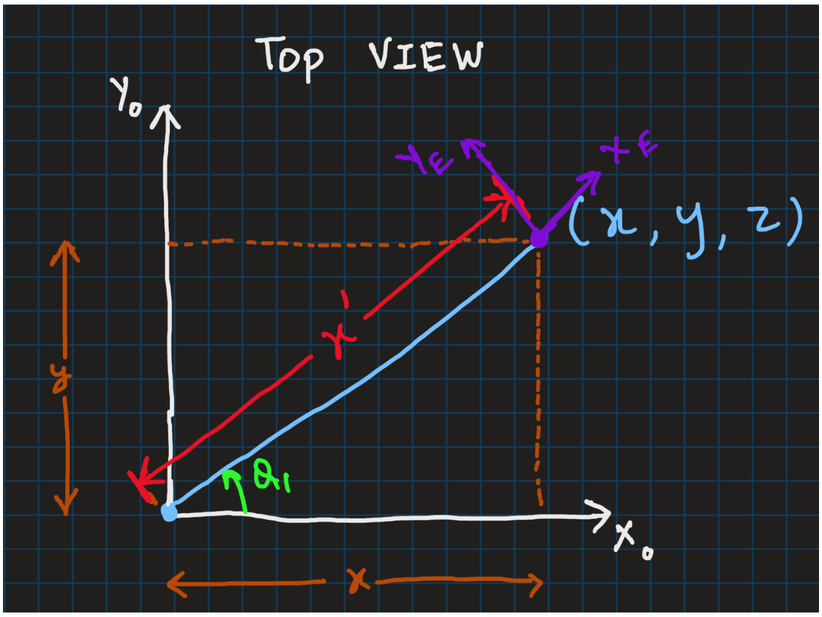

Figure 8: Top View of the robot

3.1.2 Q_2, Q_3, Q_4 solution

In order to calculate the joint displacements Q_2, Q_3, Q_4, we will have to consider the side view of the robot arm in frame 1. This is because Q_2, Q_3, Q_4 are rotating angle about z_2, z_3, z_4 respectively which are all perpendicular to plane x_1-z_1 and have same direction. The first step is to transform the end-effector's position from frame 0 to frame 1. Using Forward Kinematics, we know the transformation matrix from frame 0 to 1, and we also know the relation of x and y (Equation 3). Therefore, the expression of the end-effector's position in frame 1 is

$$
{}^{1}_{0}T = \begin{bmatrix} \cos(Q_1) & \sin(Q_1) & 0 & 0 \\ -\sin(Q_1) & \cos(Q_1) & 0 & 0 \\ 0 & 0 & 1 & -d_1 \\ 0 & 0 & 0 & 1 \end{bmatrix}, \quad {}^{0}r = \begin{bmatrix} x \\ y \\ z \\ 1 \end{bmatrix}, \quad y = x\tan(Q_1)
$$

$$
{}^{1}r = {}^{1}_{0}T * {}^{0}r = \begin{bmatrix} x\,\cos(Q_1) + y\,\sin(Q_1) \\ y\,\cos(Q_1) - x\,\sin(Q_1) \\ z - d_1 \\ 1 \end{bmatrix} = \begin{bmatrix} \frac{x}{\cos(Q_1)} \\ 0 \\ z - d_1 \\ 1 \end{bmatrix} = \begin{bmatrix} x_E \\ y_E \\ z_E \\ 1 \end{bmatrix} \tag{4}
$$

Observing from Figure 9, the relationship between Q_2, Q_3 and Q_4 can be derived from 3 triangles, i.e., triangle BCD, BDE and DEF. Points B, C, D refer to the joints associated with Q_2, Q_3, Q_4 respectively.

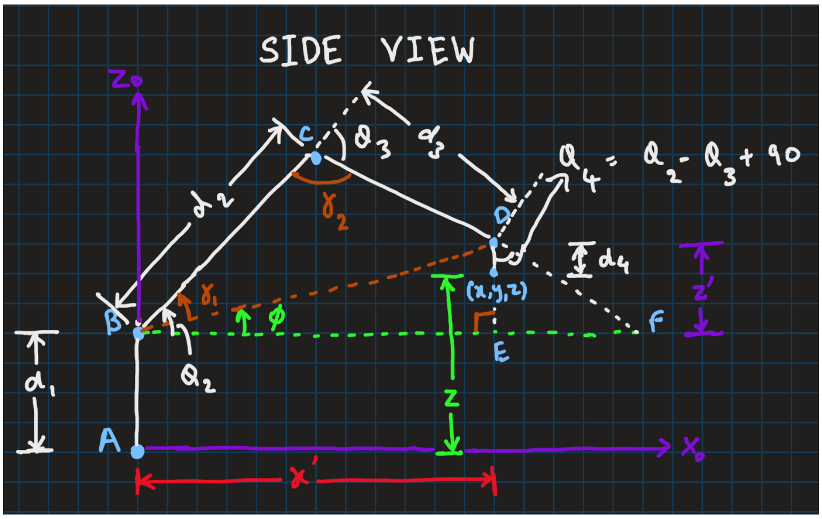

Figure 9: Side View of the robot

Considering triangle BDE and Equation 4, we can obtain the equation for z' and x' as:

$$
x' = x_E, \quad z' = z_E + d_4 = z - d_1 + d_4 \tag{5}
$$

Since z' and x' have been determined in triangle BDE, we can calculate the angle ϕ by taking the arctan:

$$
\phi = \tan^{-1}\frac{z'}{x'} \tag{6}
$$

We consider triangle BCD to determine the angles γ_1 and γ_2 by applying sine and cosine rule respectively.

$$
\cos\gamma_2 = \frac{d_2^2 + d_3^2 - (x'^2 + z'^2)}{2d_2d_3} \tag{7}
$$

$$
\gamma_2 = \pi - Q_3 \tag{8}
$$

Substituting Equation 7 into Equation 8 to solve for Q_3, we obtain:

$$
Q_3 = -\cos^{-1}\frac{(x'^2 + z'^2 - (d_2^2 + d_3^2))}{2d_2d_3} \tag{9}
$$

Observing Equation 9, it is obvious that there are 2 values of Q_3 that satisfy the equation. The two solutions form the '*elbow up*' and '*elbow down*' configuration where Q_3 respectively has negative and positive value. For this application, only '*elbow up*' will be appropriate. Therefore, from Equation 9, only values from the third and forth quadrant will be valid.

Applying the sine rule to triangle BCD for solving γ_1, adding with ϕ, we obtain the value of Q_2 as

$$\frac{\sin\gamma_1}{d_3} = \frac{\sin\gamma_2}{\sqrt{x'^2 + z'^2}} \implies \gamma_1 = \sin^{-1}\frac{d_3\sin\gamma_2}{\sqrt{x'^2 + z'^2}}, \qquad Q_2 = \phi + \gamma_1 \tag{10}$$

To determine the value of Q_4, we consider the outermost triangle BCF and DEF. By applying the property of exterior angle tringle to BCF, we obtain:

$$\begin{aligned} Q_3 &= Q_2 + [180 - (90 + Q_4)] \\ \therefore Q_4 &= Q_2 - Q_3 + 90 \end{aligned} \tag{11}$$

In Equation 11, we treated Q_3 and Q_4 as absolute angle. In order to have the end-effector always pointing down, Q_4 will be always negative of the absolute value.

Overall, we have obtained the values of Q_1, Q_2, Q_3, Q_4 respectively, given the x, y and z position of the end-effector in frame 0. Since we have two values for Q_3, there are 2 sets of solution for each configuration. However, only the angles that form the '*elbow up*' configuration is considered to be valid.

3.2 Inverse Kinematics Verification

This part aims to verify the Inverse Kinematics solution. This is conducted by selecting 2 specific locations to place a give piece on the chessboard (r_1, r_2) and calculating the joint space solutions associated with each of the locations using the determined link length from the previous section. The first location r_1 = [170;0;10;1] is chosen and its inverse kinematics solutions are shown in Table 4 and visually demonstrated in Figure 4.

Table 4: Inverse Kinematics Results for r_1 = [170;0;10;1]

Case	Q_1	Q_2	Q_3	Q_4	**End-effector pose (x,y,z) in frame 0**		
1	0	-0.85	1.81	-2.54	170	0	10
2	0	0.96	-1.81	-0.72	170	0	10

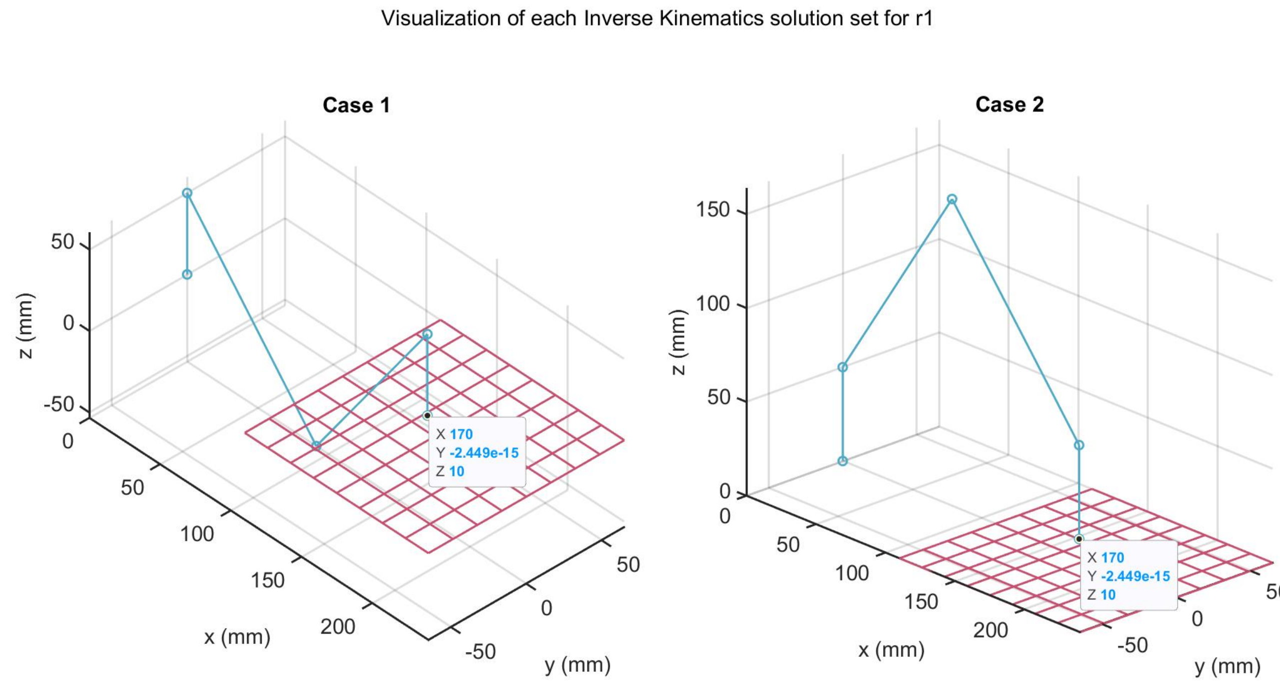

Figure 10: Inverse Kinematics Results for r_1

There are 2 different solution sets of the joint displacement from input r_1 in the space (Table 4 and Figure 10). Case 1 and 2 are '*elbow down*' and '*elbow up*' manifold respectively, which also gave the correct location of the end-effector. However, for this such application, we will only consider '*elbow up*' manifold and Case 2 presents the correct Inverse Kinematics solution set of the given location r_1.

Similarly for r_2, the solution sets are presented in Table 5 and Figure 11 where Case 2 gave the correct end-effector pose in the inertial frame. Since Case 1 is '*elbow down*' manifold, Case 2 will be slected as it is '*elbow up*' manifold and presents exactly the configuration of the robot arm to reach to the given location r_2.

Table 5: Inverse Kinematics Results for $r_2 = [110;65\ ;20;1]$

Case	Q_1	Q_2	Q_3	Q_4	**End-effector pose (x,y,z) in frame 0**
1	0.53	-0.93	2.17	-2.81	110 65 20
2	0.53	1.24	-2.17	-0.64	110 65 20

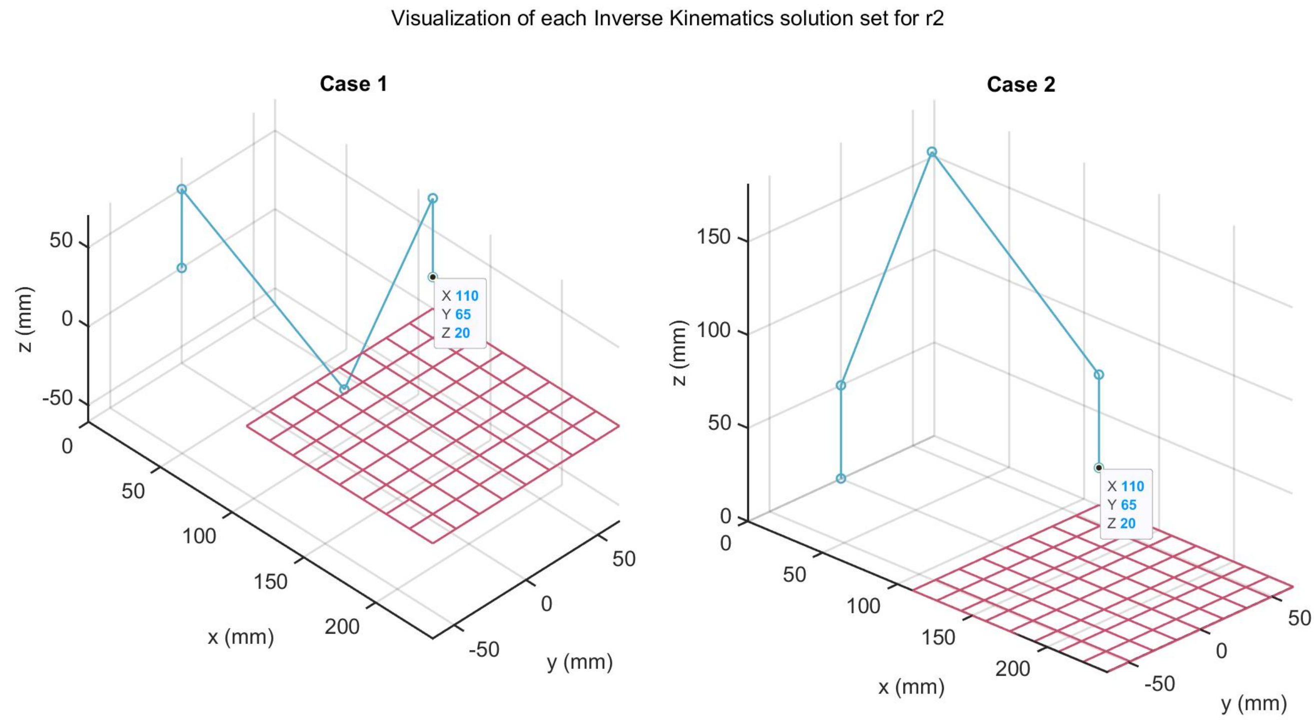

Figure 11: Inverse Kinematics Results for r_2

Furthermore, 5 different critical locations on the chessboard have been assessed to verify the capability of the robot arm and Inverse Kinematics solution. These locations are 4 corners of the board and the closest location to the robot arm, visualised in Figure 12, 13, 14.

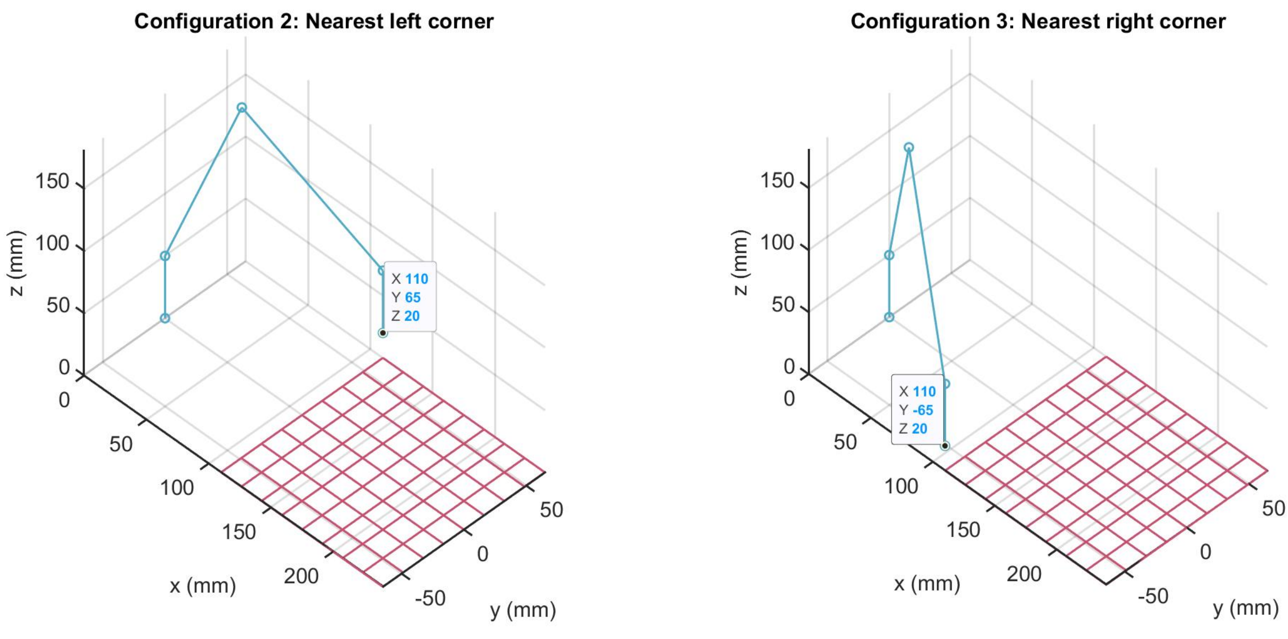

Figure 12: Configuration 2 and 3

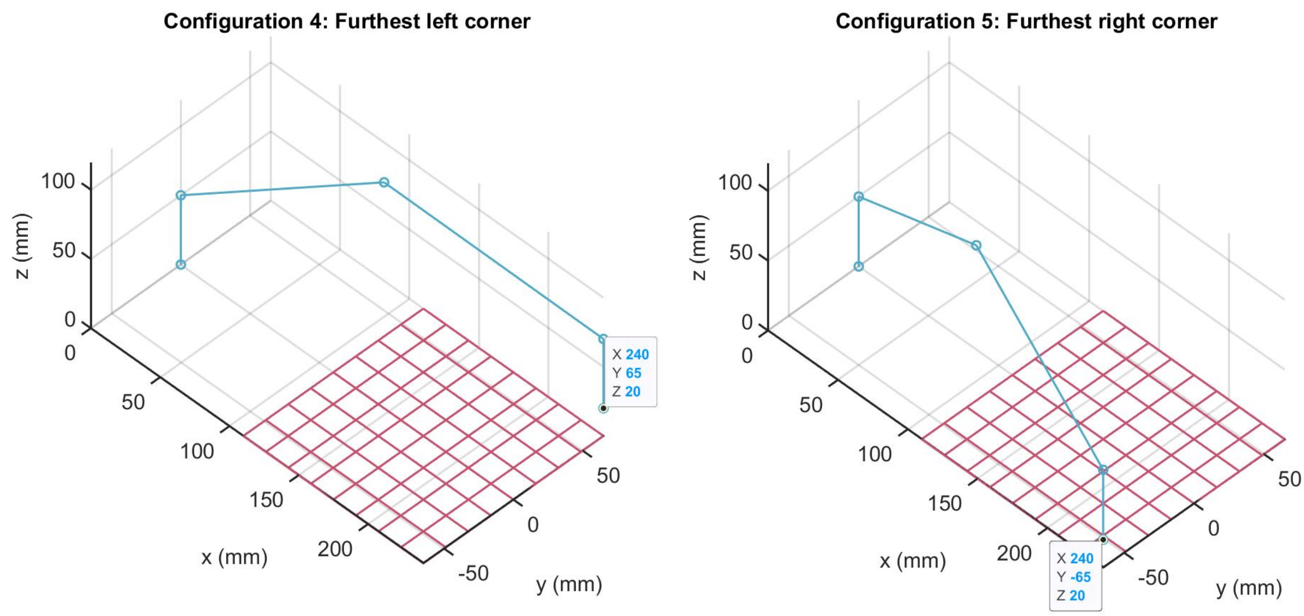

Figure 13: Configuration 4 and 5

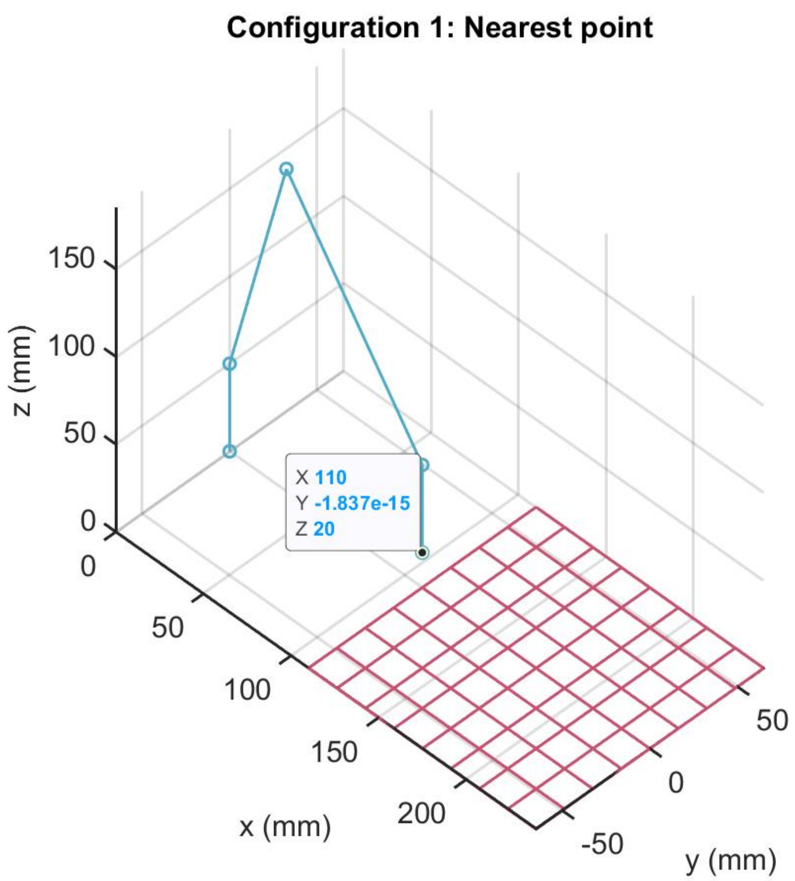

Figure 14: Configuration 1

4 Conclusion

This report covered the forward kinematics using the Denavit-Hartenberg conventions to determine robotic arm link-lengths that would cover every location on the chessboard for picking and dropping the chess pieces. From there, inverse kinematics was used to verify that with the chosen link length, the chessboard is fully covered in the workspace. MATLAB plots were plotted to verify the results of Forward Kinematics, determined link lengths and Inverse Kinematics solution.

References